AFCRL-63-450

PERFORMANCE CHARACTERISTICS AND EMISSION COOLING MEASUREMENTS
TAKEN ON A Cs VAPOR THERMIONIC CONVERTER
WITH A THORIUM-TUNGSTEN EMITTER

J. M. Houston

General Electric Company
Research Laboratory
Schenectady, New York

Contract No. AF-19(604)-8424

Project No. 8659

Task No. 865902

Scientific Report No. 1

May 1963

Prepared

for

Requests for additional copies by Agencies of the Department of Defense, their contractors, and other Government agencies should be directed to the:

DEFENSE DOCUMENTATION CENTER
ARLINGTON HALL STATION
ARLINGTON 12, VIRGINIA

All other persons and organizations should apply to the:

U. S. DEPARTMENT OF COMMERCE
OFFICE OF TECHNICAL SERVICES
WASHINGTON 25, D. C.

ABSTRACT

Measurements were made on a cylindrical, indirectly heated Cs-vapor thermionic converter having a stainless steel collector spaced 1 mm from a 13.3 cm^2 Th-W emitter. At an emitter temperature of 2100° K a power output of 4.4 watts/cm^2 (at 1.3 volts) at a measured over-all efficiency of 8.5 per cent was observed. At 2200° K, a power output of 8.8 watts/cm^2 at 11.9 per cent efficiency was observed. Measurements of the cooling of the emitter due to electron emission indicate that in the retarding range of the converter the emission cooling is just what simple theory would predict, the plasma electron temperature being equal to that of the emitter. However, for collector-to-emitter voltages more positive than approximately -1.3 volts, the emission cooling fell far below that predicted by simple electron emission from the emitter, indicating that a large amount of power (as much as 20 watts/cm^2 at positive collector voltages) was flowing from the plasma back to the emitter. This anomaly in the emission cooling is interpreted in terms of resonance radiation, excited atoms, and ions returning to the emitter. These originate in a region of high electron temperature adjacent to the emitter.

TABLE OF CONTENTS

LIST OF ILLUSTRATIONS

PERFORMANCE CHARACTERISTICS AND EMISSION COOLING MEASUREMENTS TAKEN ON A Cs VAPOR THERMIONIC CONVERTER WITH A THORIUM-TUNGSTEN EMITTER*

J. M. Houston

I. INTRODUCTION

The present research had two goals. The first goal was to investigate the power output and efficiency that would be achieved in a Cs thermionic converter using a thorium-dispenser cathode (i. e., a noncesiated emitter). Because Cs vapor is not used for modification of the emitter work function in this converter, a Cs pressure of only 10^{-2} to 10^{-1} torr is sufficient to neutralize electron space charge and to lower the collector work function. In contrast, cesiated-emitter converters require much higher Cs pressures, i. e., typically several torr. As a consequence of this low Cs pressure, plasma losses are low, output voltage is high (1. 1 to 1. 4 volts), and there is no need for very close spacing (i. e., a 1-mm gap was used in the present work). Converters using Th-W emitters have been built previously under this program,[1, 2] the maximum power output and efficiency previously observed being 4. 2 watts/cm^2 and 7. 5 per cent at T_E = 2160°K. The converter studied in the present research is the first in which the collector temperature could be optimized, the previous Th-W devices having collectors which operated near the cesium reservoir temperature. As would be expected, optimizing the collector temperature (to minimize the collector work function) improved the output, the present device yielding 4. 4 watts/cm^2 at a measured over-all efficiency of 8. 5 per cent at T_E = 2100°K, and 8. 8 watts/cm^2 at 11. 9 per cent efficiency at T_E = 2200°K. It is felt that emitter life should be relatively long at 2100°K, i. e., in an earlier test one such converter was operated 400 hours at approximately 2160°K without decay in the power output. However, we do not yet know what the emitter life will be at 2200°K.

The second goal of this research was to measure carefully the emission cooling of the emitter which occurs when large currents are drawn from the thermionic converter. These measurements are of interest because they allow one to estimate the power flowing from the plasma back to the emitter and thus are another approach by which plasma processes in a Cs thermionic converter can be studied. A previous measurement[3] had indicated that the emission cooling is anomalously low during arc-mode operation. The present more precise measurements, made over a range of emitter temperatures and Cs pressures, confirm this anomaly. As will be later discussed, this anomaly is caused by resonance radiation, excited atoms, and ions flowing from the plasma back to the emitter.

---

*This work is related to that performed under previous contract No. AF-19(604)-5472, reported under Scientific Report No. 1 of that contract, May 1960.

II. EXPERIMENTAL TUBE AND APPARATUS

The experimental tube is shown in Fig. 1. The emitter consists of a porous sintered tungsten cylinder (OD = 0.599 inch, ID = 0.4880 inch, length = 1.100 inch, density = 16.0 g/cm^3) which had been impregnated with a small amount of thorium metal. Both the OD and the ID of the W cylinder were carefully ground to true cylinders before impregnating with Th. The outer surface of the cylinder was also polished to a shiny finish. The W cylinder was slipped over a carefully machined tantalum cylinder (OD = 0.4875 inch, ID = 0.462 inch) which served as the vacuum envelope for the bombardment chamber. A thin section (0.187 inch long, 0.004 inch wall) was machined into the Ta cylinder adjacent to the emitter to serve as an "optimum lead." Inside the Ta sleeve was a tungsten bombardment filament (described in detail in the Appendix) which was used to heat the emitter by radiation and electron bombardment. Both the top and bottom of the bombardment chamber were fitted with several layers of heat-shielding (0.001-inch Ta foil) to minimize stray heat losses. After initial evacuation, the bombardment chamber was permanently sealed off from the pumps.

By occasionally evaporating a little Ti in an attached getter bulb, the pressure in the bombardment chamber was kept in the 10^{-9} to 10^{-5} torr range at all times.

The collector was made of type 347 stainless steel and had a highly polished interior surface with an ID of 0.680 inch, the emitter-collector gap thus being 1.0 mm. The emitter surface could be viewed through a sapphire window and an 0.081-inch-diameter hole in the collector. A magnetically operated nickel shutter was located adjacent to the window to keep materials evaporated by the emitter from darkening the sapphire window. However, this proved to be a needless precaution since there was never the slightest evidence of window darkening, even on the portions of the window not protected by the shutter. A heater-tape was wrapped around the sapphire window in order to maintain its temperature above that of the Cs reservoir and prevent Cs condensation.

The metal-ceramic seal was composed of a Lucalox-type high-alumina ceramic (99.5 per cent Al$_2$O$_3$) brazed to 0.010-inch Ni sheet. An

ONE INCH

TO ION GAUGE AND Ti GETTER

SAPPHIRE WINDOW

STAINLESS COLLECTOR

TO CESIUM RESERVOIR

Fig. 1 Experimental Cs thermionic converter 6A.

additional layer of Ni was incorporated into the seal as ʳ ᴜard ring to allow the elimination of leakage currents when measuring small r   erse currents in the diode. A thermal impedance (plus a cooling tube) was inᴄ ⸱ ᵃted into the collector so that the seal could be run cooler than the collectᵣ ⸱ However, to date that feature has never been used, the seal being operateᴅ ᵤt close to collector temperature.

The Cs reservoir was initially made completely from nickel. However, after encountering difficulties with the vacuum-tightness of squeezed-off Ni tubing, this was changed to a fernico and glass reservoir which has proved to be completely satisfactory at the relatively low reservoir temperatures used in this research. When we first operated the experimental tube we found that the reservoir temperature was being affected by the collector temperature (via heat conduction down the connecting tubing). To prevent this we clamped on a "buffer" oven part way down the tubing which was operated about 50 degrees hotter than the Cs reservoir and served to decouple the collector and Cs reservoir. Both the "buffer" oven and the Cs reservoir oven had their own automatic temperature controllers. The Cs oven incorporated a large piece of heavy brass tubing in close proximity to the glass reservoir so that the Cs reservoir was held at a uniform temperature. A Chromel-Alumel thermocouple was used to measure the Cs reservoir temperature. By virtue of these refinements the Cs reservoir temperature could be held constant (within a few tenths of a degree) for as long as desired.

In this research the emitter and collector temperatures, T_E and T_C, were independently varied over wide ranges. To achieve high values of T_C (e. g., 700°K) at low values of T_E (e. g., 1400°K) it was necessary to add glass-wool insulation to the collector. At high values of T_E (e. g., 2200°K) it was necessary to cool the collector. This was done by spraying the outside of the collector block with several small jets of air carrying a mist of distilled water. The water evaporated instantly when it struck the collector, but carried away much heat in the process. This "mist" cooling proved to be quite convenient and easy to adjust. We controlled the collector temperature manually, but by adding a solenoid-controlled air valve the control could easily have been made automatic.

All emitter temperatures quoted in this report were determined with an optical pyrometer, the brightness temperatures being converted to true temperatures by assuming the spectral emissivity of tungsten plus a small correction for the sapphire window transmission.

Figure 2 gives the circuits which were used to take 60-cycle current-voltage characteristics and for steady-state operation. Various modifications of these circuits were also used. For instance, when small back-currents were being measured (e. g., ion currents or collector thermionic emission) the collector was operated at negative potentials and the guard-ring connection on the metal-ceramic seal was used. All the meters shown in Fig. 2 were high-quality mirror-scale meters with accuracies of 1/2 per cent or better. In addition, we carefully calibrated several of the meters, e. g., the ones used to measure I and V, and corrected the data for the slight meter errors.
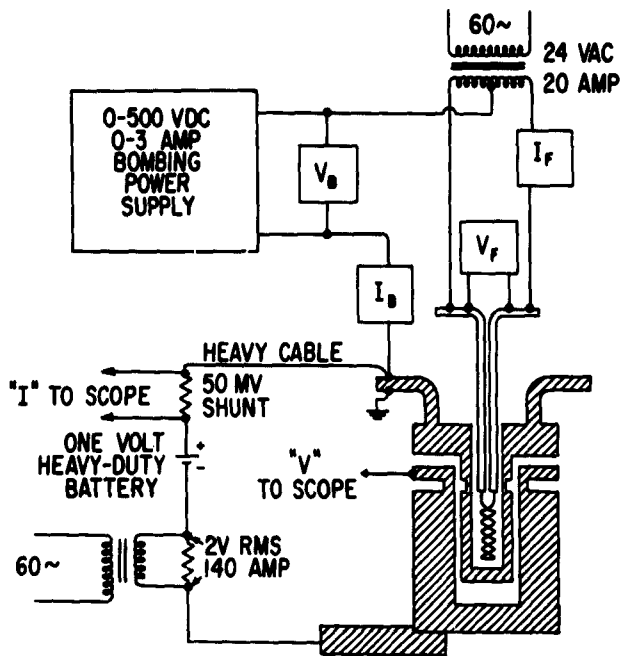
(a) Circuit used for 60 cps I-V data.
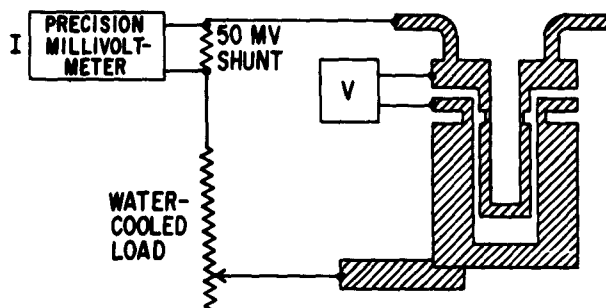
(b) Circuit used for steady-state data.

Fig. 2 Circuits used for heating the emitter and for either operating steady state or sweeping the collector voltage at 60 cps.

During the emission cooling measurements it was necessary to alternate between open-circuit and various resistive loads, the emitter being returned to precisely the same temperature before each data point was read. It is the author's experience that this can only be done to an accuracy of about ± 10 degrees using an optical pyrometer, and it is a very tiring and qualitative process. A 10-degree error causes about a 10-watt error in the resultant power input, and causes a large scatter in the emission-cooling data.
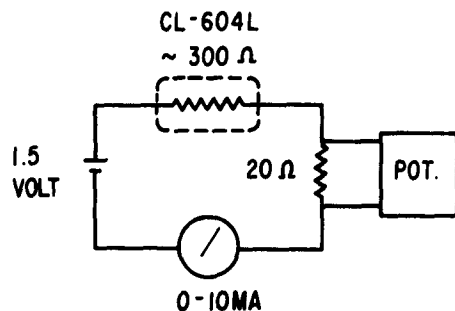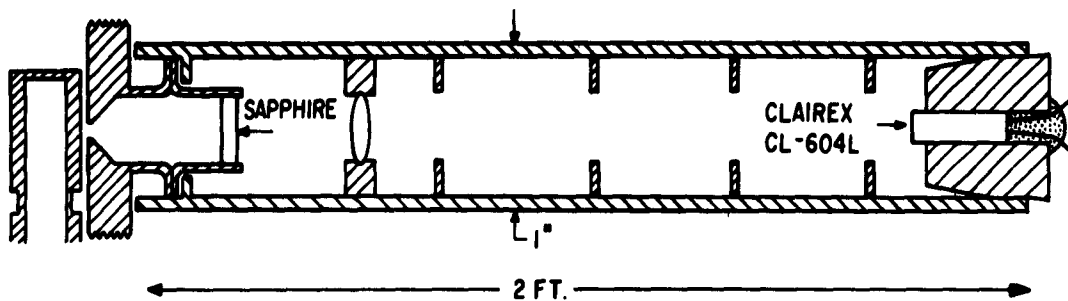
Fig. 3 Photoresistor apparatus and circuit used to hold emitter temperature
  constant during emission cooling runs.

In order to avoid this problem the photodiode apparatus of Fig. 3 was
assembled. In this apparatus an image (enlarged five times) of the emitter light
passing through a 0.081-inch hole in the collector, is projected onto a CdSe
photoconducting cell. The image more than covers the photodiode so alignment
is not critical. The photodiode is quite sensitive, so a simple, inexpensive lens
(diameter = 1.6 cm, focal length = 9.8 cm) is adequate. Because the photo-
diode is not very temperature sensitive at the light fluxes (about 10 footcandles)
used in this experiment, no temperature stabilization was used. The photodiode
electrical circuit is also shown in Fig. 3. A stable source of voltage must, of
course, be used.

The photodiode was used as follows. Before each emission cooling run
the power input conditions necessary to reach a given emitter temperature (at
open-circuit) were noted. Then the pyrometer was removed, the photodiode put
in its place, and the emitter returned to the desired temperature by precisely
duplicating the power input conditions. The current flowing in the photodiode
circuit was next read by balancing the potentiometer. The potentiometer setting
was then left unchanged during the remainder of the run, the power input to the
converter being adjusted to bring the potentiometer galvanometer to a null at
each data point. The 10 ma meter was used to get close to the null before keying

the potentiometer. In this manner one can easily and rapidly return to very nearly the same emitter temperature at each data point.

With this circuit one could readily detect a 0.1 degree change in emitter temperature (corresponds to 1 mm deflection of potentiometer galvanometer) but the stability of our power sources was such that we only attempted to hold the emitter temperature constant to within one degree. This proved to be quite easy after we equipped the bombing supply with "coarse" and "fine" voltage adjustments. The photodiode circuit did exhibit a steady drift of the order of a few degrees per hour, perhaps because it was not temperature controlled. However, in emission cooling measurements one is only interested in short-term stability since one goes back and forth between open-circuit and various loads. Thus this drift was not a problem.

III. CURRENT-VOLTAGE CHARACTERISTICS, POWER OUTPUT, AND EFFICIENCY

In order to survey quickly the performance of tube 6A we took current-voltage (hereafter denoted I-V) data over a wide range of emitter and reservoir temperatures using a 60 cps voltage sweep and oscilloscope photography. The results are shown in Fig. 4. In the constant-current region of many of the I-V characteristics taken at the lower Cs pressures, one sees a blurred region that is due to the occurrence of radiofrequency oscillations. The behavior of oscillations in this type of thermionic converter has been described previously[4] and will not be repeated here. At the higher Cs pressures one also notes discontinuities in the I-V characteristics corresponding to a discontinuous jump into "arc mode" operation.

All the I-V data of Fig. 4 (except for T_r = 573° K) are taken at the optimum collector temperature which was measured at each reservoir temperature. At T_r = 573° K, the collector temperature was a few degrees below optimum, but the difference is negligible, i.e., ϕ_c was within 0.01 volt of its optimum value. In Fig. 5 these optimum collector temperatures are shown for the present device (tube 6A) and for a similar earlier device (tube 4) which had a copper collector and a glass envelope. Note that the optimum T_c values vs T_r are not very different for the two tubes. There is considerable scatter in the data because the work-function minimum is broad, i.e., there is a range of the order of ± 30 degrees around the optimum T_c where ϕ_c is within 0.01 volt of optimum.

The value of the optimum ϕ_c was determined by several techniques, i.e., analysis of the retarding range of low-pressure I-V curves and by direct measurement of collector thermionic emission (assuming a Richardson "A" of 120). Both of these techniques yielded ϕ_c = 1.8 volts at optimum T_c. It is interesting to note, however, that the optimum ϕ_c found for tube 4 (by the same techniques) was 1.5 volts. It is not obvious why the two tubes differ since the collectors in both tubes are known to be covered with many monolayers of evaporated thorium. Presumably some gaseous impurity in tube 4 caused the difference.

Figure 6 is a plot of log (short-circuit current density) vs reciprocal emitter temperature, the J values being taken from Fig. 4. Also plotted are the Richardson lines (A = 120 amp/cm^2 °K^2) for ϕ_E = 3.3 and 3.4 volts. A value of ϕ_E = 3.35 volts is a reasonable fit to the data. At T_r = 348° and 374°K the J values fall below this line (at high T_E) because of ion limiting of the converter current. It is difficult to take good data on this ion limitation at low Cs pressures because, as the collector or other miscellaneous parts of the tube warm up, they give off Cs and the diode current can temporarily go to much higher values than the true ion-limited value determined by the Cs reservoir. However, at T_r = 348 °K we did take pains to wait until these spurious Cs pressures had died away. The dashed lines on Fig. 6 are plots of 492 J_p, where J_p was calculated from the Langmuir-Saha equation for surface ionization and 492 is the square root of the Cs atom-electron mass ratio as required by simple, collisionless space-charge neutralization. As can be seen, the observed electron
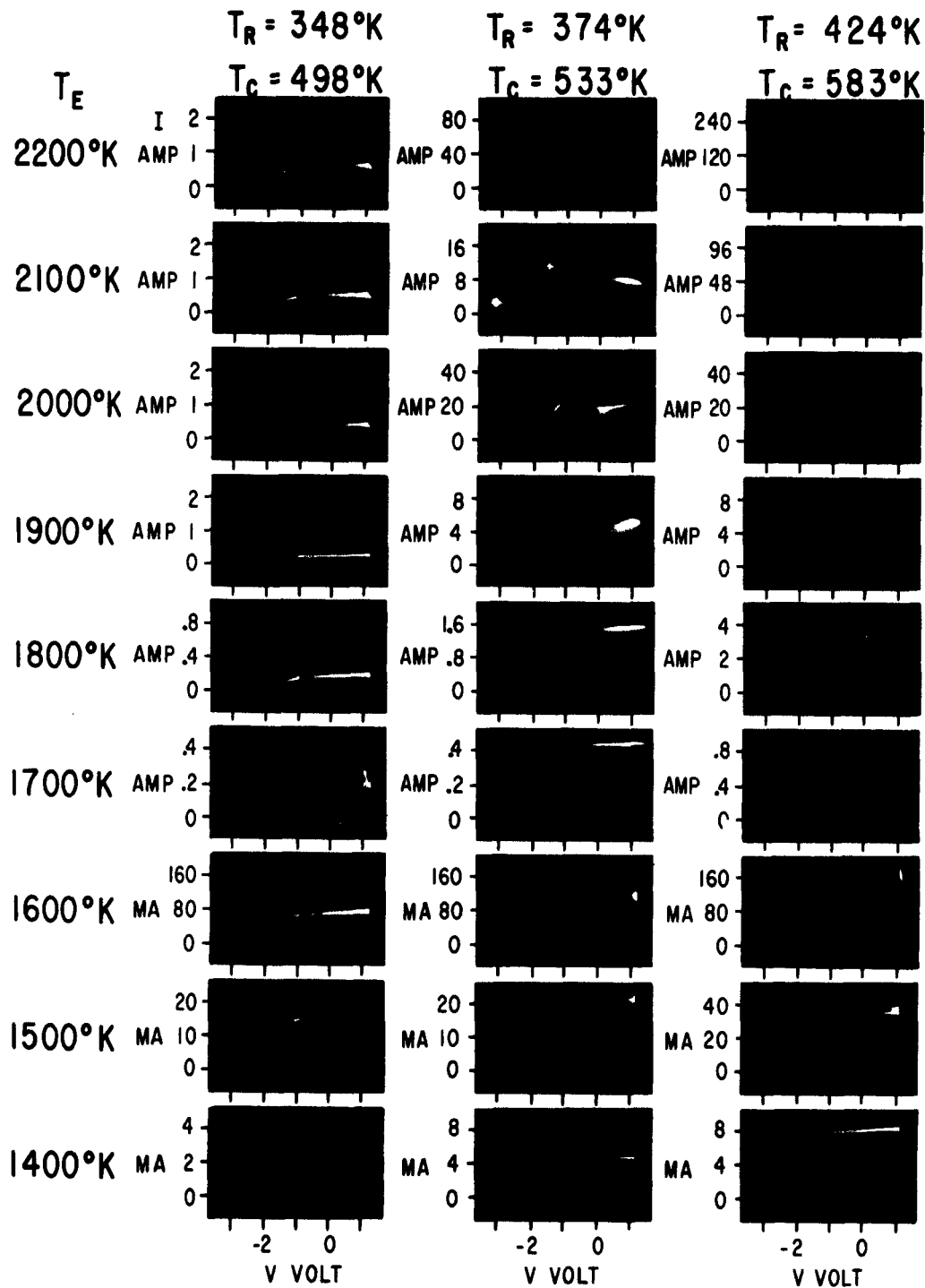
Fig. 4 Current-voltage characteristics taken with the 60 cps voltage
sweep.
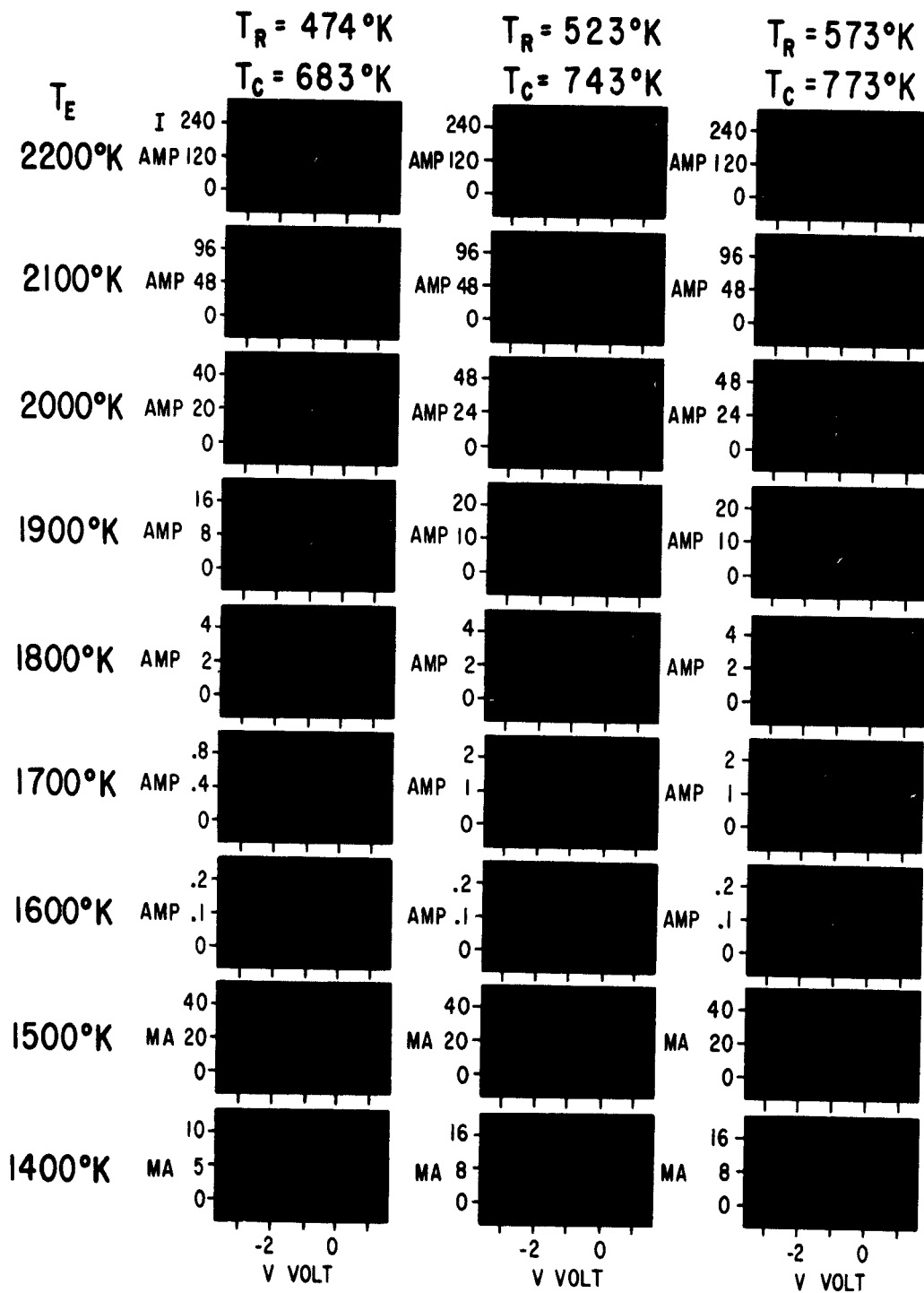
Fig. 4 (continued).
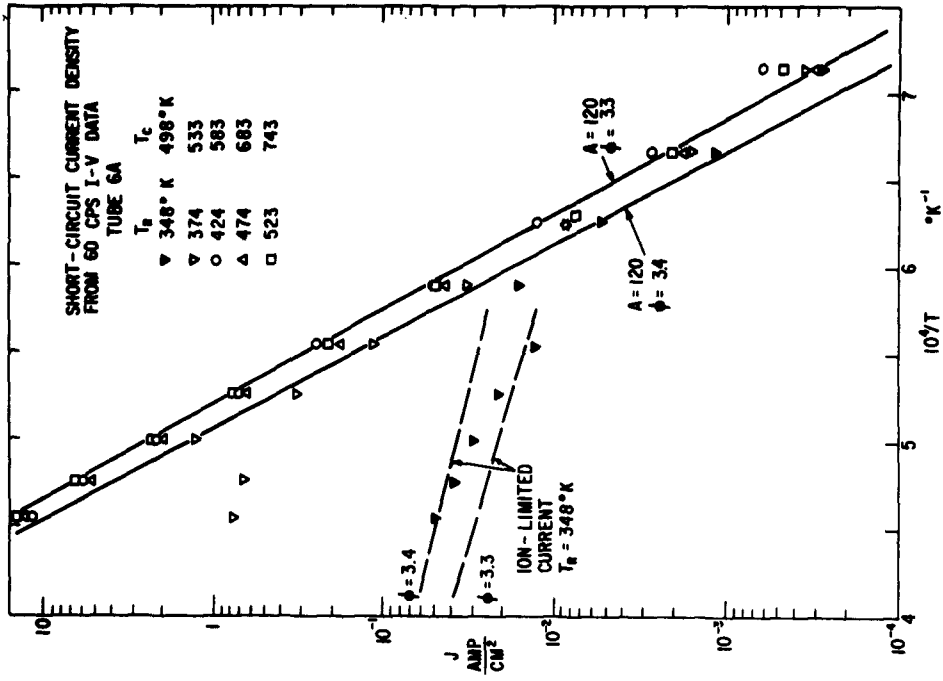
Fig. 6 Short-circuit current density from Fig. 4 plotted vs reciprocal emitter temperature.
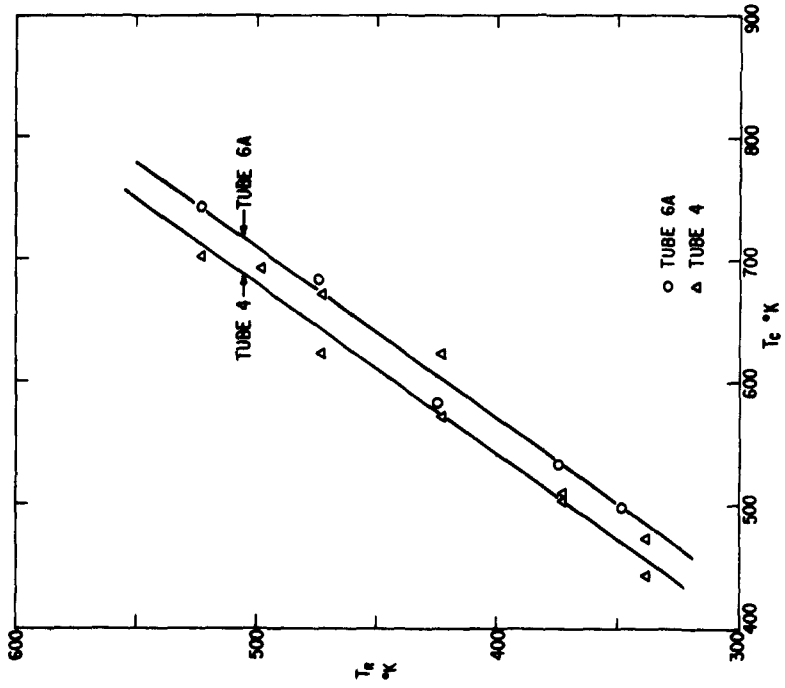
Fig. 5 Optimum collector temperature vs Cs reservoir temperature.
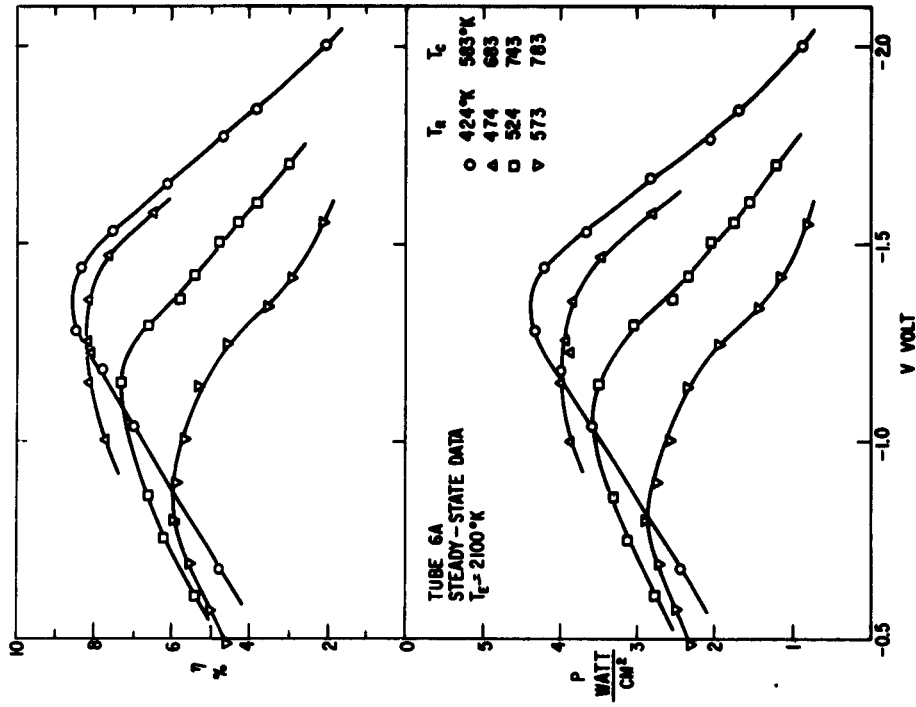
Fig. 9 Power output and efficiency vs converter voltage at $T_E = 2100\,°K$.
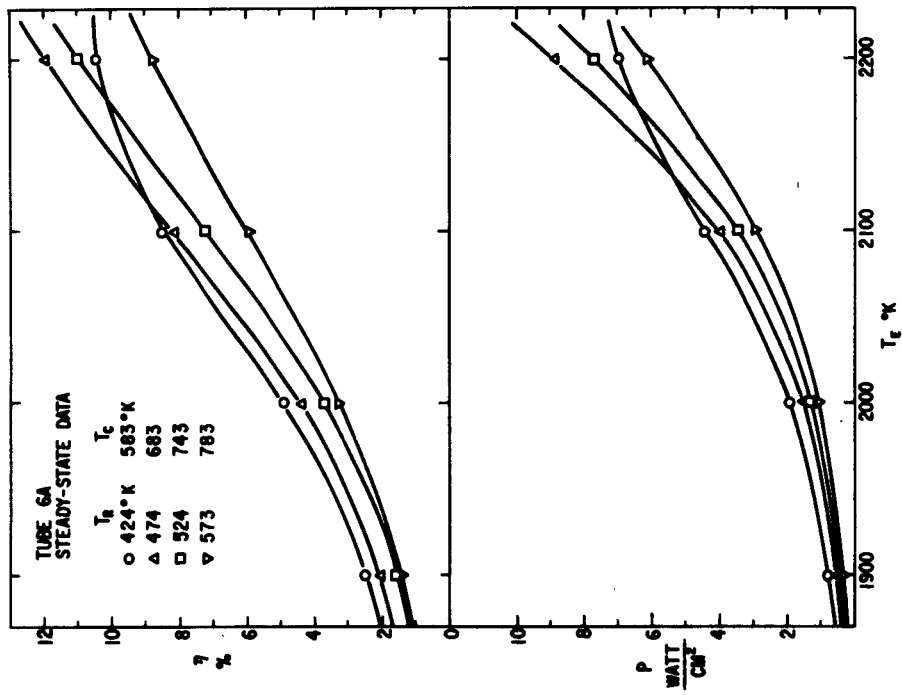
Fig. 8 Steady-state power output and measured over-all efficiency as a function of emitter temperature.

IV. EMISSION-COOLING MEASUREMENTS

As explained in the Introduction, the purpose of these measurements was to explore the anomalously low emission cooling which occurs in the arc mode. The philosophy of these measurements is as follows: Hold the emitter temperature constant (so that all stray losses, e.g., radiation and heat conduction, will remain constant) and measure the required power input both under load and at open circuit. The difference between the "load" and "open-circuit" power inputs is then just that due to emission cooling (or heating) effects as a result of current leaving (or arriving at) the emitter. The experimental results can be interpreted in terms of a mixed flow of particles, e.g., electrons leaving the emitter and ions (or excited atoms) arriving at the emitter.

The measurements were made using the circuit of Fig. 2(b), except that during part of each run the water-cooled load was replaced with a storage battery so that the measurements could be extended into the region where the collector is positive with respect to the emitter.

As explained in Section II, a photodiode was used to hold the emitter temperature constant to within about 1 degree, which corresponds to a random uncertainty in power input of about 1 watt. The collector temperature and Cs reservoir temperature were also held constant during a run. The measurements were made by measuring the power input at various load currents, returning to measure open-circuit power input after every two or three data points. Successive open-circuit measurements of P_{in} usually agreed to within 1 watt although there was sometimes a slow, regular drift in open circuit P_{in} values (presumably due to photodiode drift) which amounted to about a 5-degree drift in T_E during the entire run. This much of a change in T_E is insignificant. The change in T_E between a "load point" and its adjacent open-circuit points (which were used to calculate ΔP) was always much less than 5 degrees. Several runs were repeated to check the data for reproducibility. The runs always agreed well (e.g., see Fig. 10). For typical values of input power, etc., see Table A-I in the Appendix.

The quantity $\Delta P/I$ was plotted where I is the converter current and ΔP is the net emission cooling given by the following expression:

$$\Delta P = P_1 + I^2 R_0 - P_0 . \tag{1}$$

Here P_1 and P_0 are the power input under load and at open circuit, respectively, and the $I^2 R$ term is a small correction added because the load current does produce a little ohmic heating of the emitter (and of the thin "optimum lead") which thus slightly reduces the value of P_1 that would otherwise have been measured. It can easily be shown that for a uniformly emitting cylindrical emitter:

$$R_0 = (R_t/2) + (R_e/3) \tag{2}$$

where R_t is the resistance of the thin "optimum lead" and R_e is the end-to-end resistance of the emitter itself. This correction is very small, e.g., for a typical data point where I = 51.7 amperes, the values of the quantities in Eq. (1) were P_1 = 676.4 watts, P_0 = 481.2 watts, and $I^2 R_0$ = 1.4 watts.

Note that there is one more possible source of resistance, namely the interface between the Ta support cylinder and the W emitter. If this resistance were even as large as 20 milliohms, it would completely upset the emission cooling measurements at high values of I. For this reason a careful analysis of this resistance was made which is given in the Appendix. This analysis indicates that this contact resistance is negligible.

The measured values of $\Delta P/I$ for $T_E = 2000°K$ are plotted in Figs. 10, 11, and 12, and for $T_E = 2100°K$ in Figs. 13, 14, and 15. The values of collector-to-emitter voltage are shown beside each experimental point. The solid line drawn on each of these figures is the theoretical emission cooling one would expect if the diode current were all electrons flowing from emitter to collector. This line was calculated by assuming the Richardson equation with an A value of 120 amp/cm^2°K^2, as follows:

$$J = 120\, T_E^2\ \exp\,(-eV_k/kT)\ . \tag{3}$$

From this equation one can calculate a barrier height, V_k, as a function of I. The emission cooling when emitting electrons over this barrier is given by:

$$(\Delta P/I) = V_k + (2\,kT_E/e)\ . \tag{4}$$
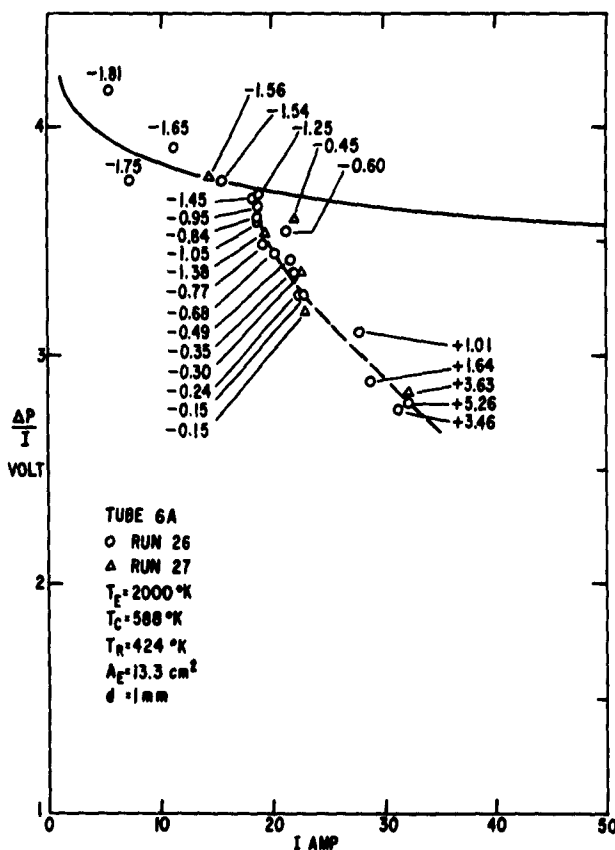
Fig. 10 Emission cooling data taken at T_E = 2000° and 2100°K for three different Cs reservoir temperatures. The solid line is the theoretical prediction for simple electron flow from emitter to collector.

Fig. 12

$\dfrac{\Delta P}{I}$ VOLT

-1.70
-1.76
-1.75
-1.62
-1.57
-1.54
-1.43
-1.29

-1.33
-1.23
-1.15
-1.05

-1.05
-0.95
-0.80
-0.59
-0.41
-0.21
-0.07

+1.46
+1.51

+3.05
+3.07

TUBE 6A
RUN 37
$T_E = 2000°K$
$T_C = 723°K$
$T_R = 524°K$
$A_E = 13.3 \ cm^2$
$d = 1 \ mm$

I AMP
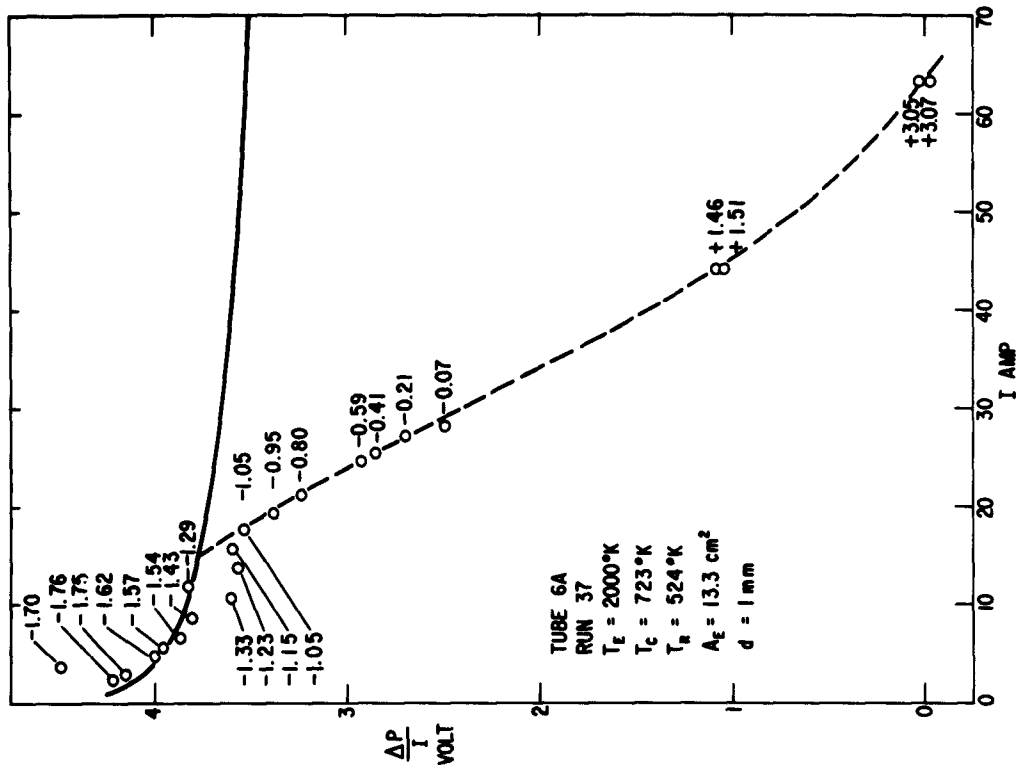
Fig. 12 Same as Fig. 10.

Fig. 11

$\dfrac{\Delta P}{I}$ VOLT

-1.18
-1.28
-1.40
-1.50
-1.55
-1.69
-1.75
-1.85

ARC MODE

-1.05
-0.89
-0.70
-0.55
-0.40
-0.18
-0.06
-0.06

+1.65
+1.66

+3.48
+3.51 VOLT

TUBE 6A
RUN 32
$T_E = 2000°K$
$T_C = 683°K$
$T_R = 474°K$
$A_E = 13.3 \ cm^2$
$d = 1 \ mm$

I AMP
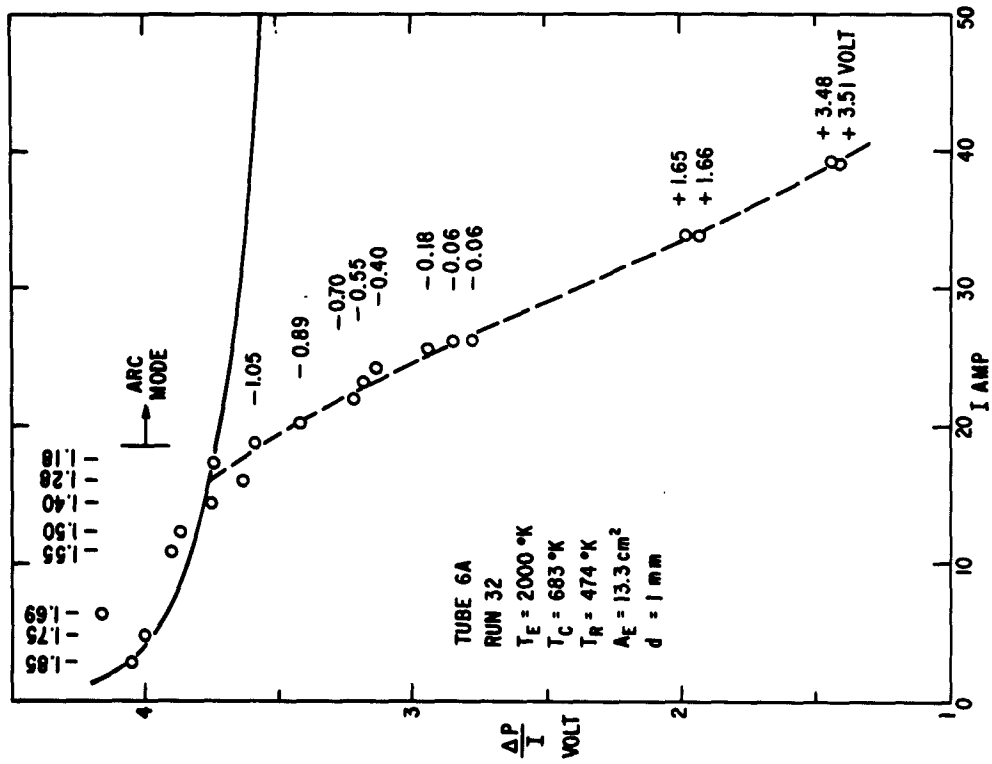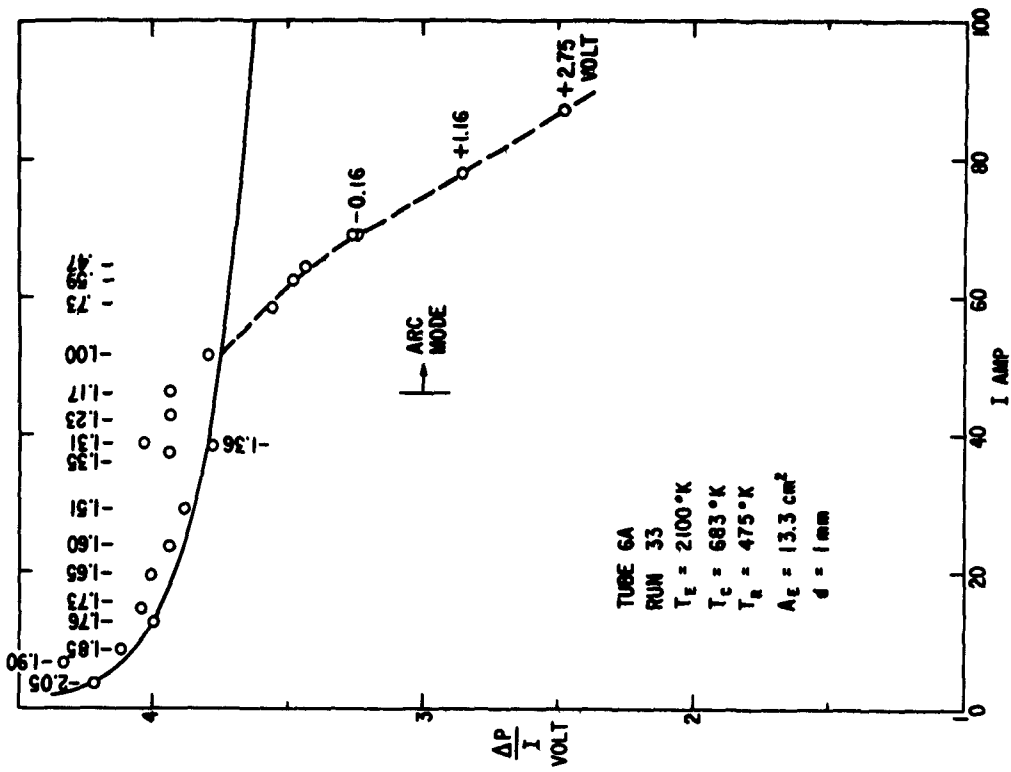
Fig. 11 Same as Fig. 10.

Fig. 14 Same as Fig. 10.
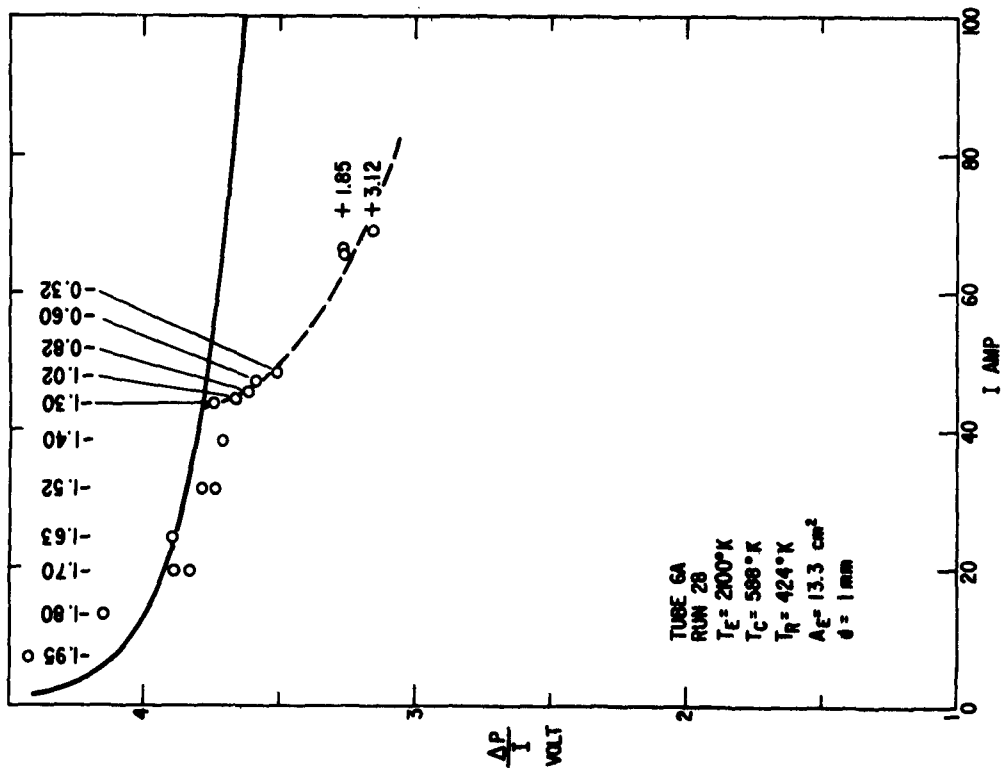
Fig. 13 Same as Fig. 10.

Fig. 15 Same as Fig. 10.

TUBE 6A
RUN 38
$T_E = 2100°K$
$T_C = 723°K$
$T_R = 524°K$
$A_E = 13.3 cm^2$
$d = 1 mm$

Data point labels: 1.94, 1.86, 1.80, 1.70, 1.61, 1.56, 1.50, 1.42, 1.36, 1.30, -2.01, -1.15, -0.86, -0.75, -0.61, -0.18, +0.70, +0.77, +1.05, +1.65

Axis: $\frac{\Delta P}{I}$ VOLT ; I AMP
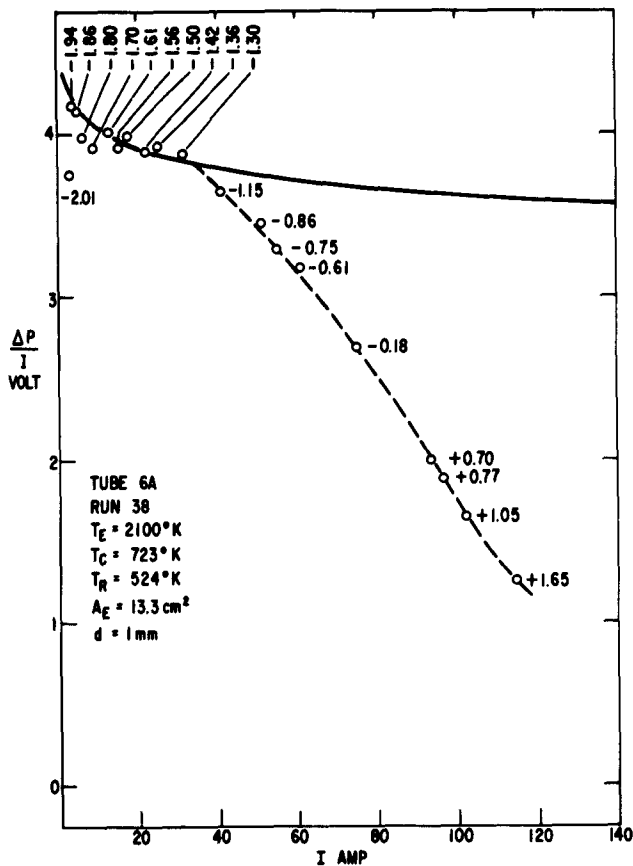
Note that, in general, the experimental points agree well with the solid line at
small values of I but fall far below the solid line at large values of I. The
scatter in the experimental points becomes larger at small values of I, merely
because, as mentioned earlier, there is a random measurement error of about
1 watt in ΔP. This produces a random error in $\Delta P/I$ which increases at small
values of I, i.e., is about 0.2 volt at I = 5 amperes and only 0.02 volt at
I = 50 amperes.

The fact that the measured $\Delta P/I$ values agree with the simple theory at
small values of I is in accord with the motive diagram shown in Fig. 16(a).
Here (for all the T_r values of Figs. 10 through 15) there is an ion-rich emitter
sheath in accord with the predictions of the Langmuir-Saha equation and the
experimental observations on ion-limiting shown in Fig. 6. The barrier which
determines the diode current, I, is at the collector, i.e., the diode is in the
retarding range. The saturated electron emission of the emitter flows into the
plasma, much of this current flowing back to the emitter from the plasma. The
electron temperature in the plasma is very close to that of the emitter, as the
energy balance in the plasma requires it should be.

When V is reduced to the order of -1.3 volts, the $\Delta P/I$ values begin
to fall below the solid line predicted by simple theory. The dashed lines in
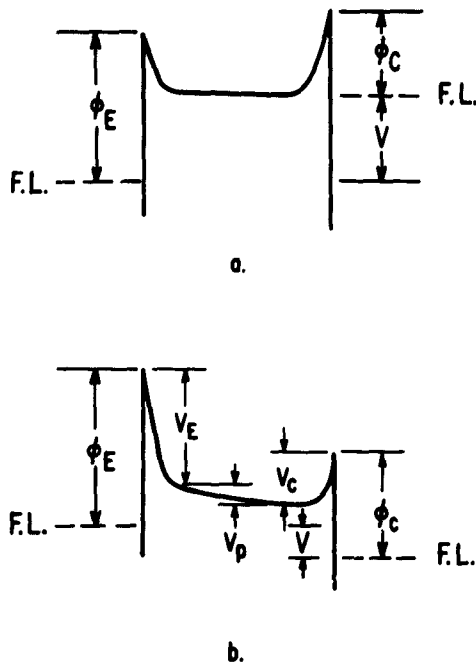
Fig. 16 Motive diagram for the converter in the retarding range (case a) and for arc mode operation (case b).
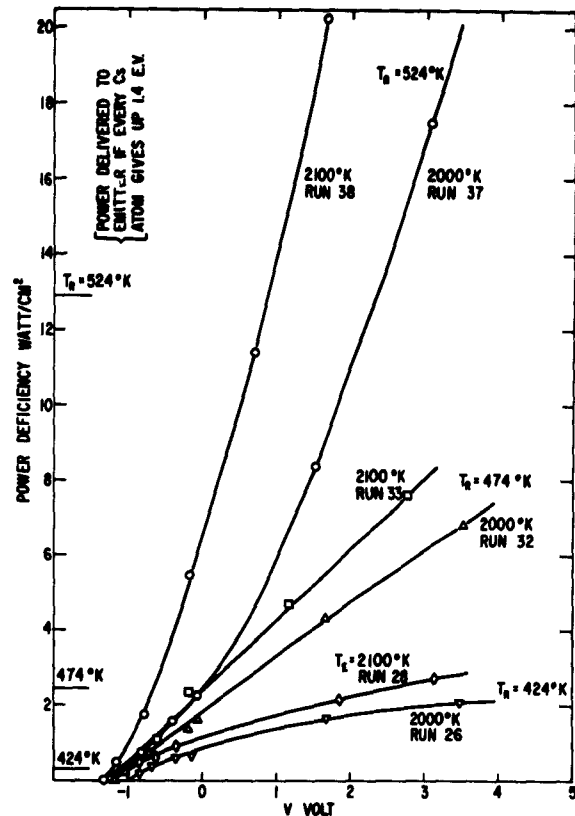
Fig. 17 Plot of the discrepancy between the experimental points and the solid lines drawn on Figs. 10 through 15.

Figs. 10 through 15 were arbitrarily drawn in as a reasonable fit to the experimental points. Figure 17 is a plot of the power deficiency (expressed in watts/cm^2), i.e., the difference between the solid curves and the dashed curves in Figs. 10 through 15. Note that the power deficiency increases rapidly as Cs pressure increases, and is as high as 20 watts/cm^2 at T_r = 524°K.

Note that the power deficiency is still present (although smaller) at relatively low Cs pressures, i.e., T_r = 424°K (see Figs. 10 and 13). During these two runs noisy fluctuations were present in the diode current for values of V > -1.3 volts. These fluctuations, which are certainly related to the coherent oscillations seen at this Cs pressure at slightly lower values of T_E, looked like white noise on an oscilloscope being swept at 50 μsec/cm. They could not be synchronized or "stopped" on the oscilloscope under any conditions. The band of noise had an amplitude of approximately 1 volt, centered about the d-c value of V which was read with a meter. The noise peaks never extended into the retarding range of the diode, however. No fluctuations were noted in the current during emission cooling measurements made at the higher Cs pressures (i.e., Figs. 11, 12, 14, 15) in accord with earlier observations of oscillations in this type of converter. [4]

The decrease noted in the $\Delta P/I$ values is due basically to the fact that power is somehow being fed back from the plasma to the emitter. Various mechanisms are possible. One possibility is energy feedback via high-temperature electrons which flow back to the emitter from the plasma. This effect will exist, but is far too small to explain the observed anomaly. For instance, an electron which is emitted at 2000°K and returns at 5000°K contributes only 0.52 ev to the emitter. Furthermore, as V becomes more positive, the current flowing from the plasma to the emitter must diminish (i.e., is small compared to I even at short circuit) whereas the anomaly grows.

Another highly probable mechanism is the flow of excited Cs atoms back to the emitter. For instance, most theories of the "arc mode" postulate that the first excited state in the Cs vapor (1.4 volts above the ground state) is densely populated. At the left-hand side of Fig. 17 is indicated the power which would flow to the emitter if every neutral Cs atom striking the emitter yielded 1.4 ev to the emitter. Here the flux of Cs atoms was assumed to be μ_a, the value calculated from gas kinetics. One sees that excited atoms could explain nearly all of the anomaly in the power-output quadrant of the I-V curve (i.e., for V < 0). However, the anomaly gets too large to be explained by excited atoms for V > 0.

Another mechanism which almost certainly is occurring is the flow of Cs ions from the plasma to the emitter. These ions recombine at the emitter and heat rather than cool the emitter. The current I at the emitter is thus made up of an electronic and an ionic component, I_e and I_p. The ions are created by volume ionization in the Cs vapor adjacent to the emitter, i.e., the so-called "arc-mode."

In order to get an idea of the magnitude of the ion currents which would be required, the data of Figs. 10 through 15 were interpreted assuming the entire anomaly is due to ion current. The motive diagram of Fig. 16(b) is used in this calculation, where V_E and V_c are the emitter and collector sheath voltages [assumed to be positive when having the polarity shown in Fig. 16(b)], and V_p is the ohmic drop in the plasma. This is the motive diagram usually employed in explaining low-voltage arcs, and is in agreement with experimental observations.[5, 6] Note that the diode is now definitely not in the retarding range, the barrier determining the electron flow in the diode now being ϕ_E.

Each ion flowing from the plasma to the emitter contributes an energy $V_E + (V_i - \phi_E)$ to the emitter, where V_E is the emitter sheath down which the ion falls and $(V_i - \phi_E)$ is the recombination energy which is assumed to be delivered to the emitter as heat. The thermal energy of the ion is ignored since the neutral atom carries away approximately the same thermal energy when it leaves the emitter. The net emission cooling of the emitter can thus be written:

$$\Delta P = I_e(\phi_E + 2kT_E/e) - I_p(V_E + V_i - \phi_E) . \qquad (5)$$

Since $I = I_e + I_p$, Eq. (5) can be rewritten (after algebraic manipulation):

$$\frac{I_p}{I} = \frac{(\phi_E + 2kT_E/e) - (\Delta P/I)}{V_E + V_i + 2kT_E/e} . \qquad (6)$$

In order to use Eq. (6) one must know V_E, the emitter sheath. Since direct knowledge of the emitter sheath is lacking, one must estimate it in some manner. By adding up potentials in Fig. 16(b), one can write

$$V_E = \phi_E - \phi_c + V_c - V_p + V \ . \tag{7}$$

Thus an estimate of V_E can be made if V_c and V_p can be estimated. Here the probe measurements of Morgulis and Marchuk[6] in a low-voltage, hot-cathode Cs-vapor arc are most useful. They found, at $T_r = 523°K$ and in the range $J = 1.7$ to 7 amp/cm^2, that a uniform electric field of 0.4 to 0.5 volt/cm was present in the plasma and that V_c was very small, e.g., 0.1 to 0.2 volt. At a spacing of 1 mm, this electric field would give rise to $V_p \sim 0.05$ volt. Therefore, both V_c and V_p were neglected in the present experiment, the two terms tending to cancel anyhow. It should be noted [see Eq. (6)] that one does not need a precise value of V_E to estimate I_p, i.e., a 1-volt error in V_E would typically cause only a 20 per cent error in the resulting I_p value.

By inserting Eq. (7) (with $V_c - V_p = 0$) into Eq. (6) one can calculate (I_p/I) values from the measured values of $\Delta P/I$. Note, however, that the numerator of Eq. (6) must vanish (because $I_p = 0$) where the dashed lines on Figs. 10 through 15 join the solid lines. Thus, by reading the $(\Delta P/I)$ values at the intersection points, one can get an independent check on the value of ϕ_E, since at the intersection point ϕ_E must equal $(\Delta P/I)-2kT_E/e$. Table I gives the values of ϕ_E determined by this method. It is seen that they average 3.4 volts which is in reasonable agreement with the Richardson data plotted in Fig. 6, especially when one remembers that the true short-circuit electron current (at high J values) may be slightly less (10 to 20 per cent) than that plotted in Fig. 6 because of ion current.

TABLE I

	T_E (°K)	$\Delta P/I$ (volt)	$2kT_E/e$ (volt)	ϕ_E (volt)
Fig. 9	2000	3.71	0.35	3.36
10	2000	3.75	.35	3.40
11	2000	3.76	.35	3.41
12	2100	3.78	.36	3.42
13	2100	3.75	.36	3.39
14	2100	3.82	.36	3.46

If one assumes $\phi_E = 3.4$ volts, $\phi_c = 1.8$ volts, $V_i = 3.89$ volts, and assumes an average value of $T_E = 2050°K$ in the unimportant kinetic energy terms, Eqs. (6) and (7) become:

$$\frac{I_p}{I} = \frac{3.75 - (\Delta P/I)}{V + 5.84} \ . \tag{8}$$

By the use of Eq. (8), a value of ion current was calculated for each value of $\Delta P/I$ in Figs. 10 through 15, the equation being valid in the region where the
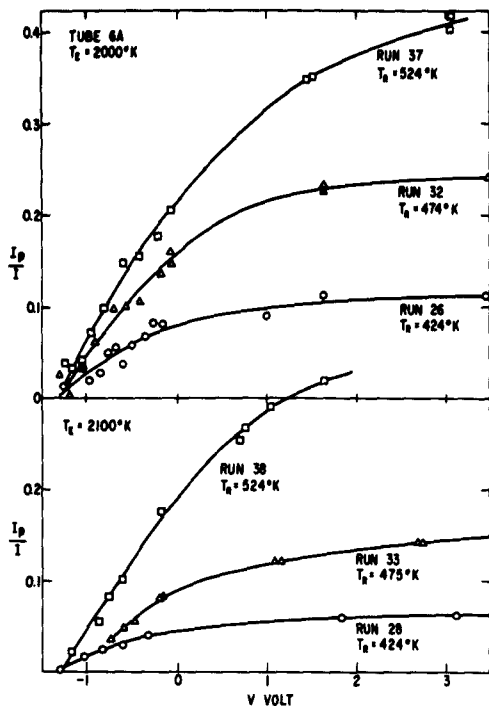
Fig. 18 Ratio of ion current to total current as a function of converter voltage. To obtain these values the entire emission-cooling anomaly was assumed to be due to positive ions.
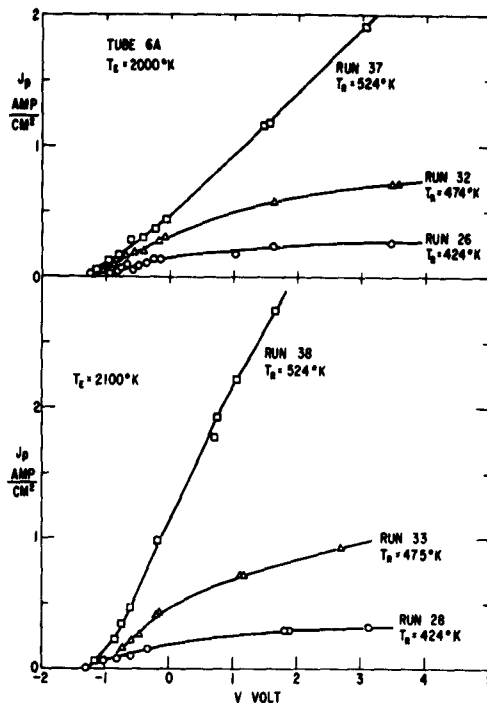
Fig. 19 Ion current density vs converter voltage.

dashed lines of Figs. 10 through 15 diverge from the solid lines. The results of these calculations were plotted in three ways. In Fig. 18 are shown the resulting values of I_p/I as a function of V. In Fig. 19 the ion current density is plotted. Note that J_p rises rapidly as V becomes more positive, especially at high Cs pressures. The J_p values also rise somewhat as T_E is increased, but in general not as fast as J_e increases. As a result, the I_p/I values tend to be a little higher at T_E = 2000°K than at 2100°K.

In Figs. 20 and 21 are shown the experimental I-V characteristics (circles) taken in the course of several emission-cooling runs, as well as the electron-current-vs-voltage characteristic (triangles) determined by subtracting I_p from I. It is seen that I_e continues to increase as V becomes more positive, but at a slower rate than I increases.

Also shown in Figs. 20 and 21 are careful tracings (solid lines) of the 60 cps I-V data from Fig. 4. These were taken on a different day from the point-by-point data, and there is no guarantee that ϕ_E or T_E was precisely the same in the two sets of data. At T_r = 474°K, the 60 cps and point-by-point data agree well except at positive voltages for T_E = 2100°K. At T_r = 424°K the 60 cps and point-by-point data agree well in the retarding range (where there are no
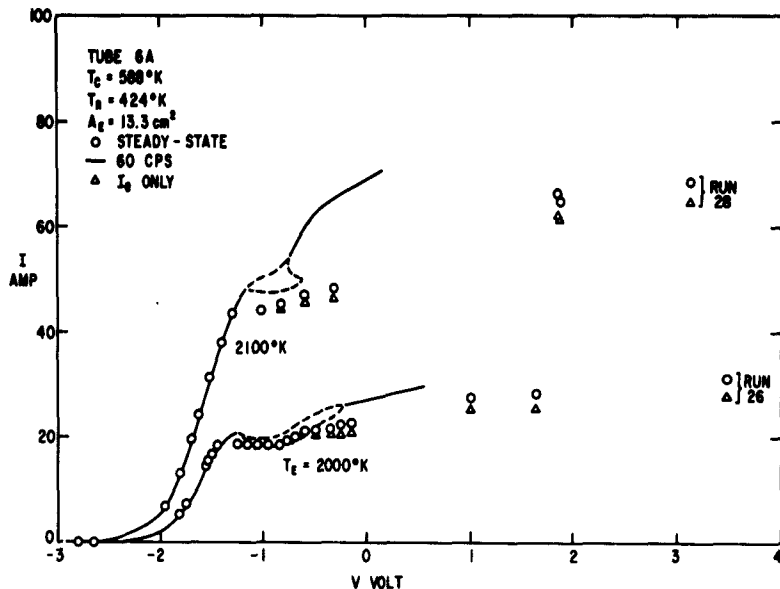
Fig. 20 Measured steady-state and 60 cps I-V plots. The dashed line bounds the oscillation region in the 60 cps characteristics. Noisy nonsynchronized oscillations were present at all the steady-state points to the right of the "knee" of the I-V curve. The triangles give the electron current only, i.e., total current minus ion current.
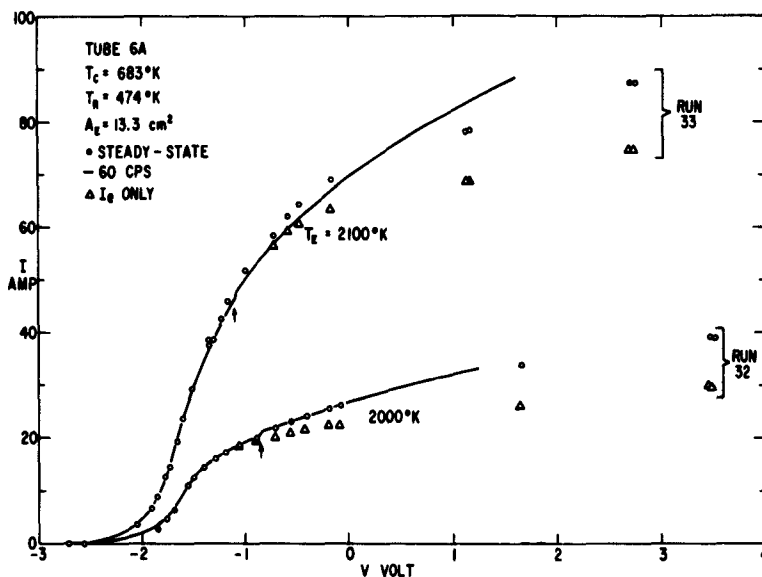
Fig. 21 Measured steady-state and 60 cps I-V data. No oscillations were observed. The arrows show a small step in the I-V curve which is believed to be the transition into the arc mode. The triangles give the electron current only, i.e., total current minus ion current.

oscillations) but disagree at more positive voltages where the noisy oscillations were noted. This is not surprising because, once oscillations are present, the I-V characteristic depends strongly on the impedance of the load or voltage source. In the case of the very-low-impedance 60 cps sweep, the oscillations appeared only in a narrow voltage range (dashed region) whereas they were present in all the point-by-point data for $V > -1$ volt. From these data (and from measurements of 60 cps and steady-state power output) we conclude that, for this device, there is little difference between 60 cps and steady-state data.

The J_D values resulting from this experiment are surprisingly high, and one cannot help but wonder: "Are these results valid, i.e., could some spurious phenomenon be going on which causes the anomalously low values of emission cooling?" One good method of checking this is to compare results with other experiments. Unfortunately there appear to be no similar experimental studies made on Cs thermionic converters. However, one paper by Morgulis and Marchuk[6] was found in the Ukrainian Journal of Physics which describes a study of a hot-cathode low-voltage Cs-vapor arc discharge. Though the contact potential and spacing are quite different from the present experiment, the results can be compared if account is taken of these differences.

In the Morgulis-Marchuk experiment a planar cesiated-Mo emitter was used, spaced 30 mm from a Mo collector. Typical operating conditions were $T_r = 523°K$, $T_E = 1040°$ to $1120°K$, and $J = 1.7$ to 8 amp/cm^2. Their measurements indicate that $\phi_E = 1.5$ volts at low current densities, and drops to 1.3 volts at the higher J values. By means of a movable probe they measured V_E, V_p, and V_c. By measuring the emitter heat balance they determined L_D/I ratios, using essentially the same assumptions and equations as given in this report.

In comparing the Morgulis results with the present experiment one must include the fact that contact potential (i.e., $\phi_E - \phi_c$) was quite different in the two experiments. Also in the Morgulis experiment a plasma drop, V_p, of the order of 1.5 volts was present (because of the wide spacing). The plasma drop should be very much smaller in the present work. For this reason the best way to compare the results is at the same V_E values, since it is primarily the emitter sheath voltage (and the current density) which will determine the rate of volume ionization. Figure 22 is a plot of the I_D/I values deduced by Morgulis and Marchuk vs their measured value of emitter sheath. They made two calculations of I_D/I, one (curve α) in which the recombination heat was not assumed to enter the emitter, and one (curve α') in which it was.

Also shown in Fig. 22 is the $T_r = 524°K$ data from Fig. 18. To convert V values to V_E for this plot, Eq. (7) was assumed with $\phi_E = 3.4$ volts, $\phi_c = 1.8$ volts, and $V_c - V_p = 0$, as discussed previously. The numbers on the curves of Fig. 22 are the measured current densities. Both experiments happen to have been done at about the same J values. One sees that, although the agreement is not perfect, both experiments yield the same general result. This strongly suggests that a real effect is being measured, and that both experiments are observing the same phenomenon.
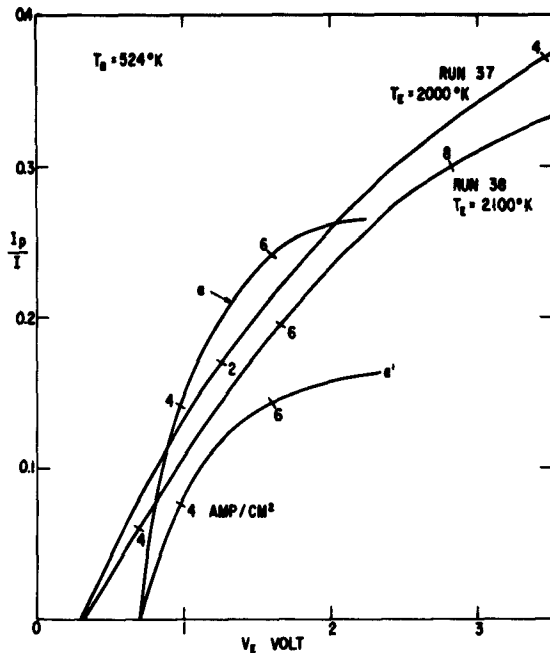
Fig. 22 Comparison of I_p/I ratio vs emitter sheath height, from the present experiment (runs 37 and 38) and from Morgulis and Marchuk.[6] The numbers on the plot are the current densities at various points along the curve.

Three mechanisms (electrons, excited atoms, and ions) have been discussed which can feed power back to the emitter from the plasma. A fourth mechanism exists, namely, radiation. As Mohler[7] has shown, most of the photon energy in a Cs plasma is carried by the two resonance lines (8521 A and 8943 A). The absorption distance is also very short (e. g., 10^{-3} cm) at these wavelengths, i.e., the plasma is optically dense. In order to estimate the maximum possible magnitude of this resonance radiation the following calculation was made. The electron temperature was calculated from

$$T_e = T_E + (e/2k)(V + \phi_E - \phi_c) . \qquad (9)$$

This equation, first given by Johnson,[8] merely assumes that all of the energy the electrons gain as they are accelerated by the emitter sheath is converted into random motion. The plasma was assumed to radiate as a black body (emissivity = 1) within the line width, with zero radiation outside the line width. The radiation was calculated for an "average" wavelength (8720 A) using the line width (sum of the two resonance lines) reported by Mohler.[7] These line widths are 0.76 A, 4.5 A, and 19.6 A at $T_r = 424°$, $474°$, and $524°K$, respectively. This procedure of using an average wavelength is the same as that used by Mohler in determining the effective line widths from measured radiation intensities. The emissivity of the W emitter was assumed to be 0.45, this being about 10 per cent higher than the value found by de Vos[9] for tungsten at this wavelength to allow for the porosity of the emitter.

The power delivered to the emitter (i. e., calculated radiation intensity multiplied by emitter emissivity) is shown in Fig. 23. One notes that Figs. 23
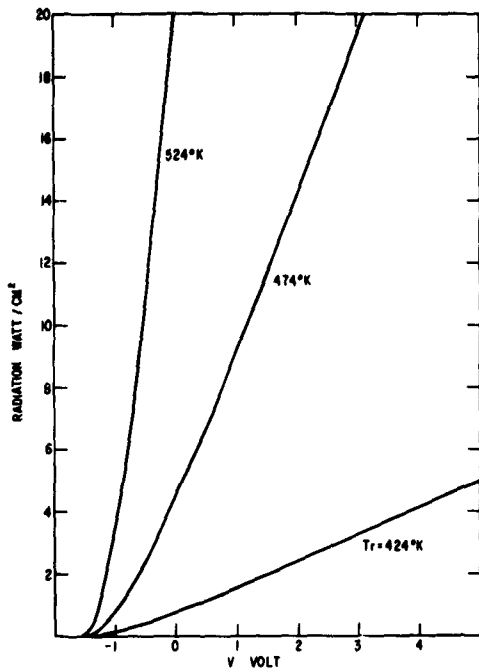
Fig. 23 Calculated maximum possible resonance radiation delivered to the emitter assuming Mohler's values for the combined line width of the two resonance lines (8521 A and 8943 A) and assuming emitter emissivity ≈ 0.45.

and 17 (the measured power deficiency) have many similar features, except that the magnitudes in Fig. 23 are, in general, somewhat higher than those in Fig. 17. This merely indicates that the actual electron temperatures are not as high as the maximum values assumed in the calculation. If one assumes that the entire power deficiency is due to resonance radiation, an electron temperature can readily be calculated, e.g., at $T_r = 524°K$ and $T_E = 2100°K$, this calculation yields $T_e = 6800°K$ at $V = 0$ volt and $12,500°K$ at $V = 2$ volts.

V. DISCUSSION

In the previous section, four mechanisms were discussed by which power can be returned from the plasma to the emitter, i.e., electrons, excited atoms, ions, and resonance radiation. At the present preliminary stage of analysis, one cannot say with certainty just how much each of the four mechanisms contributes to the observed "power deficiency," other than to state (as discussed earlier) that neither electrons nor excited atoms are the dominant effect.

Two models can be postulated which could explain the observed emission-cooling anomaly. In the first model it is assumed that the fractional ionization in the plasma adjacent to the emitter is governed by the Saha equation. Fractional ionizations of nearly "one" result, and the power deficiency would then be primarily due to ion current arriving at the emitter. Nottingham[10] has made a detailed analysis of a model of this type.

In the second model, it is assumed that the Saha equation is not valid in the layer adjacent to the emitter because of the drainage of ions to the emitter. These atoms leave the emitter primarily as neutrals. As a result the fractional ionization in this layer is considerably lower than would be predicted by the Saha equation. Under these conditions it is possible that the power discrepancy is mainly due to the feedback of resonance radiation. This resonance radiation would mainly be delivered to the emitter (except at low Cs pressures) because the region of cooler electron temperature would prevent much of the resonance radiation from reaching the collector (analogous to a series of black-body heat-shields).

In both models it is assumed that adjacent to the emitter is a region of high electron temperature as a result of randomization of the electron injection velocity. Several authors[8,10,11] have discussed the mechanisms by which this randomization can occur. In this region of high average electron energy, copious excitation and ionization will occur. The width of this region of high electron temperature is uncertain. At low Cs pressure (or for very narrow gaps) it could well fill the entire gap. At higher Cs pressure the electron temperature will rapidly fall (due to inelastic collisions) as one moves away from the emitter, eventually falling to an equilibrium temperature in the range 2000° to 3500°K typical of the positive column of a Cs discharge.[6,7] Note that this is somewhat different from the usual published models of the arc-mode Cs converter, which invariably assume a uniform electron temperature throughout the gap.

Webster[12] has recently built a Cs converter in which he could observe the interelectrode gap (0.46 mm), i.e., look in parallel to the cesiated-W emitter surface. At $T_E = 2050°K$, $T_c = 863°K$, $T_r = 590°K$, $J = 5.7$ amp/cm^2, $V = 0.45$ volt (arc-mode operation), he observed a bright layer about 0.15 mm thick adjacent to the emitter. This layer is probably a region of higher electron temperature.

We are at present making calculations to see which model seems more reasonable. Both models have minor difficulties. For instance, one can easily calculate what ion current would strike the emitter if the plasma was completely

ionized, i. e., the number of ions/cm^2 sec was equal to μ_a, the atomic flux. At $T_r = 424°$, $474°$, and $524°$K, this ion current is 0.21, 1.72, and 9.1 amp/cm^2, respectively. However, Fig. 19 shows that at $T_r = 424°$K an ion current of up to 0.33 amp/cm^2 is required to explain the observed power deficiency. At the two higher Cs pressures, this difficulty does not occur, i. e., the ion current required to explain the power deficiency is less than that calculated for 100 per cent plasma ionization. This discrepancy at $T_r = 424°$K merely indicates that not all of the observed power deficiency can be due to ions, i. e., must be partially due to resonance radiation. The second model (power feedback mainly resonance radiation) requires very high electron temperatures, i. e., higher than have been reported for the positive column of Cs discharges. However, these measurements do not rule out the possibility of a high electron temperature adjacent to the emitter.

It is obvious that these emission cooling measurements are a new and interesting method of studying the plasma adjacent to the emitter. After further analysis has indicated which plasma model seems most reasonable (and, at the moment, model one seems more likely), the power deficiency measurements can be straightforwardly interpreted to find the electron temperature, the plasma density, and the ion current adjacent to the emitter.

VI. CONCLUSIONS

The principal conclusions of this study are:

1. At T_E = 2100°K a power output of 4.4 watts/cm^2 (at 1.3 volts) at a a measured efficiency of 8.5 per cent was observed. At 2200°K, a power output of 8.8 watts/cm^2 at 11.9 per cent efficiency was observed.

2. In the retarding range of the converter the electron temperature is essentially equal to the emitter temperature, as is required by the power flow into the plasma.

3. In the nonretarding range, the emission-cooling of the emitter falls far below that predicted by simple electron flow, indicating that a substantial amount of power (e.g., 20 watts/cm^2 at a positive collector voltage) is flowing from the plasma to the emitter.

4. This "power deficiency" is probably due mainly to ions flowing to the emitter, although excited atoms and resonance radiation will also contribute. The required ion currents are of the order of a few amp/cm^2. An ion current of this magnitude will cause a large accelerating (for emitter electrons) electric field at the emitter surface.

5. It is possible that the resonance radiation contribution to the power deficiency is larger than the ion contribution, i.e., that the power deficiency is mainly due to resonance radiation. Further analysis will settle this point.

REFERENCES

1. J. M. Houston, MIT Physical Electronics Conf. Report, 72 (March 1960).

2. V. C. Wilson, <u>Energy Conversion for Space Power</u>, N. W. Snyder, ed., Academic Press, New York (1961), p. 138.

3. J. M. Houston, MIT Physical Electronics Conf. Report, 114 (March 1961).

4. J. M. Houston, MIT Physical Electronics Conf. Report, 92 (March 1962).

5. R. K. Steinberg, J. Appl. Phys., <u>21</u>, 1028 (1950).

6. N. D. Morgulis and P. M. Marchuk, Ukrain. Fiz. Zhur., <u>2</u>, 379 (1957).

7. F. L. Mohler, Natl. Bur. Stds. J. Res., <u>9</u>, 493 (1932).

8. E. O. Johnson, R. C. A. Rev., <u>16</u>, 498 (1955).

9. J. C. DeVos, Physica, <u>20</u>, 690 (1954).

10. W. B. Nottingham, MIT Physical Electronics Conf. Report, 95 (1960).

11. W. H. Lewis, <u>Energy Conversion for Space Power</u>, Academic Press, New York (1961), p. 133.

12. H. F. Webster, GE Research Lab., private communication.

APPENDIX

ELECTRICAL RESISTANCE OF INTERFACE
BETWEEN TUNGSTEN EMITTER AND TANTALUM SUPPORT SLEEVE

In this Appendix the electrical resistance of the interface between the cylindrical tungsten emitter and the tantalum support sleeve will be analyzed and shown to be negligible. It is essential that this interface resistance be known, since if it were as large as only 2×10^{-2} ohm, an ohmic heat of 200 watts would be generated in the emitter structure when an emitter current of 100 amperes was drawn. This would be of the right magnitude to explain the observed anomalously low values of emission cooling.

The procedure which is used to determine the interface resistance is the following. First, the temperature of the tungsten bombardment filament at any steady-state point in the experimental emission-cooling measurements can be determined from its electrical resistance. From this filament temperature and the filament power input, the temperature of the Ta support sleeve (which surrounds the filament) can be deduced. One can then estimate the radiation heat transfer across the Ta-W interface, the remaining power flow being by thermal conduction through points of contact. The electrical resistance of the Ta-W interface can then be calculated since the thermal and electrical conductivities are related by the Lorenz number. In the remainder of this Appendix this procedure is described in more detail.

The bombardment filament (see Fig. 1 in main text) consists of a bifilar helix composed of approximately 12.7 inches (weld-to-weld) of 0.020-inch-diameter tungsten wire. This filament is a rather open structure, each helix having a diameter (wire-center to wire-center) of 0.231 inch and a pitch of 10 turns/inch. The length of the filament which is within the heat-shielded region (see Fig. 1) is approximately 12.4 inches. The filament is mounted on 0.060-inch-diameter Mo press leads which each have a length of 7.0 inches down to the point where the potential taps for the filament voltmeter (for measuring V_f) are attached just outside the tube. Both I_f and V_f are measured using precision meters, the values of I_f being corrected for the small amount of current drawn by the voltmeter.

After the filament had been welded to the press leads, but before it was inserted into the experimental tube, the filament was mounted in a bell jar (where it radiated to free-space) and flashed to 2800°K for several minutes. Then a careful measurement of filament resistance vs filament temperature was made, the filament temperature being determined from the Jones and Langmuir[1] tables of $I_f/d^{3/2}$ where d is the wire diameter. The same potential taps and meters were used during this measurement as were used during subsequent operation of the tube.

The surface area of the portion of the filament within the heat shield was determined to be 5.09 cm² from measured dimensions. Also values of this area could be deduced from the filament resistance (after a small

1. H.A. Jones and I. Langmuir, GE Rev., 30, 310 (1927).

correction for end effects) using the Jones and Langmuir values for the resistivity of tungsten. These were found to be 5.16 cm^2 from the 2400°K data, and 5.13 cm^2 from the 2600°K data. Therefore, a value of 5.12 ± 0.04 cm^2 was assumed for the value of A_f, the filament surface area within the heat-shielded zone.

As a check on the calibration of R_f vs T_f, we calculated the power radiated from A_f during this calibration, i.e., divided the measured filament power (minus a small end-effect and press-lead correction) by 5.12 cm^2. At T_f = 2400° and 2600°K, respectively, this procedure yielded 56.4 and 80.2 watts/cm^2, which agree well with the Forsythe and Watson[2] values of the radiation from tungsten (to free-space) of 55.7 and 80.6 watts/cm^2. Thus, our calibration of R_f vs T_f does not appear to be seriously in error, and allows us to determine T_f from the measured values of V_f and I_f.

Next, the temperature, T_s, of the tantalum support sleeve was calculated by writing a heat-balance equation for the bombardment filament. In deriving this equation, the bombardment filament was assumed to be immersed in a black-body hohlraum at temperature T_s. The equation is:

$$P_f + e_f \ \sigma \ T_s^4 \ A_f = e_f \ \sigma \ T_f^4 \ A_f + I_b(\phi_f + 2kT_f/e) \tag{A1}$$

where P_f is the filament power within the heat-shielded zone (i.e., measured filament power minus small end-effect and press-lead corrections), e_f is the filament emissivity, σ is the Stefan-Boltzmann constant, A_f is the filament area in the heat-shielded zone, I_b is the bombing current being drawn from the filament, and ϕ_f is the filament work function. The left-hand side gives the power delivered to the filament, and the right-hand side the power leaving the filament because of radiation or emission cooling (a small term since I_b was always less than 2 amperes). Note that all the terms in Eq. (A1) except T_s are known (or can be accurately estimated), so that one can solve for T_s at each steady-state operating point of the thermionic converter. Actually, there should be another term on the left-hand side of Eq. (A1) which takes account of the radiation from the filament which is scattered off the Ta sleeve and returned to the filament. Because this term was neglected, the calculated values of T_s will be somewhat higher than actually occur, but that fact merely strengthens the conclusions of this Appendix.

Table A-I gives values of T_s calculated in this manner for sample data points during several runs. The data points were chosen to include wide variations of I, V, and P_{in}. Note that even though P_{in} varies by several hundred watts (and at least 90 per cent of P_{in} must somehow be transferred across the Ta-W interface), the values of T_f and T_s rise only a few degrees. Also note that the temperature difference across the Ta-W interface is approximately 300 degrees in all the data.

The problem which must next be answered is: "How can powers of up to 600 watts be transferred across the 10.87 cm^2 area of the Ta-W interface?"

---

2. W.E. Forsythe and E.M. Watson, J. Opt. Soc. Am., 24, 114 (1934).

		Run 38 $T_E = 2100°K$ $T_c = 723°K$ $T_r = 524°K$			Run 33 $T_E = 2100°K$ $T_c = 683°K$ $T_r = 475°K$			Run 32 $T_E = 2000°K$ $T_c = 683°K$ $T_r = 474°K$		
I	(amp)	0	93.4	114.6	0	51.7	87.3	0	20.1	39.3
V	(volt)	-2.72	+0.70	+1.65	-2.72	-1.00	+2.70	-2.56	-0.89	+3.48
P_{in}	(watt)	491.0	672.6	626.6	484.0	676.4	696.7	387.6	454.0	445.0
I_f	(amp)	10.91	10.85	10.91	10.61	10.54	10.54	10.94	10.93	10.91
V_f	(volt)	13.60	13.61	13.62	13.03	13.02	13.00	13.20	13.21	13.19
P_f	(watt)	145.6	144.9	145.8	135.6	134.7	134.4	141.6	141.6	141.1
T_f	(°K)	2605	2620	2608	2573	2586	2583	2535	2539	2539
T_s	(°K)	2388	2410	2392	2360	2382	2381	2289	2297	2298

Possible mechanisms include radiation, thermal conduction through contact points, and thermal conduction through Cs vapor. The latter mechanism can be immediately ruled to be unimportant because, regardless of the gap, at the highest Cs pressure used in the measurements ($T_R = 523°K$) Cs gas conduction can carry less than 1 watt/cm^2 across a 300°K temperature difference. Radiation, on the other hand, can transfer appreciable amounts of power, calculations assuming clean-metal emissivities in the interface yielding a power flow of 155 watts for $T_E = 2100°K$ and $T_s = 2400°K$. If the tungsten surface were pessimistically assumed to have a black-body emissivity (which is very unlikely since it can be easily shown that the outer surface of the emitter has an emissivity approaching clean W), the radiation transfer equals 248 watts. Thus one concludes that radiation alone cannot transfer the required ~600 watts across the interface, and that heat conduction through contact points must be transferring at least 200 to 400 watts (depending on P_{in}).

The following model seems to fit the observations. When the emitter is initially heated to its maximum temperature of 2200°K, the tantalum sleeve expands out against the W emitter (due to the larger thermal expansion coefficient of Ta), the soft Ta stress-relieving during this process. If the emitter is then cooled to room temperature there would be a gap of several mils between emitter and sleeve. On subsequent heatups, the Ta warms up (and expands) until it is hot enough to transfer the entire input power by radiation, or until it contacts the W sleeve and transfers a portion of the power by heat conduction. That the latter is the case is shown by the preceding argument. That the latter is true is also shown by the fact that T_s increases by only 20 degrees when P_{in} changes by several hundred watts. No model involving only radiation heat transfer could explain the relative constancy of T_s and T_f.

Since the differential equations determining electrical resistance and heat conduction are identical (except for different constants) one can readily show that

$$R_i = K\rho \; \Delta T/W \qquad\qquad (A2)$$

where R_i is the interface electrical resistance, W is the thermal flow through the interface contact points, ΔT is the temperature drop across the interface, K is the thermal conductivity of the contact region, and ρ is the electrical resistivity of the contact region. In deriving this equation, K and ρ were assumed to be independent of temperature; hence values typical of the "average" temperature of the interface should be used. Both W and Ta have $K\rho$ values of approximately 6×10^{-5} watt ohm/deg at 2200°K, which is also within 20 per cent of the value predicted by the Lorenz number. Inserting W = 200 watts, ΔT = 300 degrees, and the above value of $K\rho$ into Eq. (A2) yields $R_i = 9 \times 10^{-5}$ ohm. For I = 100 amperes, the I^2R_i heating of the emitter is thus about 1 watt, which would cause the negligible shift in the $\Delta P/I$ values of 0.01 volt. Actually, the error is even smaller than this since at I = 100 amperes, the W value is more like 400 watts (since $P_{in} \sim 670$ watts and radiation $\leqslant 250$ watts). Thus one concludes that ohmic heating at the Ta-W interface can be neglected when interpreting the emission cooling measurements.

DISTRIBUTION LIST

Code	Organization	No. of Copies
AF-2	A.U. (Library) Maxwell AFB, Alabama	1
AF-12	AWS (AWSSS/TIPD) Scott AFB, Illinois	1
AF-22	AFCRL, OAR (CRXR, Mr. John Marple) L.G. Hanscom Field Bedford, Massachusetts (U)	1
AF-23	AFCRL, OAR (CRXRA) Stop 39 L.G. Hanscom Field Bedford, Massachusetts	Please ship under separate cover as they must be sent to our Documents Unit. (20 cpys).
AF-26	AFCRL, OAR (CRZH, C.N. Touart) L.G. Hanscom Field Bedford, Massachusetts	1
AF-28	ESD (ESRDG) L.G. Hanscom Field Bedford, Massachusetts	1
AF-33	ACIC (ACDEL-7) Second and Arsenal St. Louis 18, Missouri (U)	1
AF-35	NAFEC Library Branch, Bldg. 3 Atlantic City, New Jersey ATTN: RD-702	1
AF-40	ASD (ASAPRD-Dist) Wright-Patterson AFB, Ohio	1
AF-43	Institute of Technology Library MCLI-LIB., Bldg. 125, Area B Wright-Patterson AFB, Ohio	1
AF-48	Hq. USAF (AFCSA, Secretary) Washington 25, D.C.	1

Code	Organization	No. of Copies
AF-49	AFOSR (SRGL) Washington 25, D.C.	1
AF-51	Hq. USAF (AFRDR) Washington 25, D.C.	1
AF-58	ARL (ARA-2) Library AFL 2292, Building 450 Wright-Patterson AFB, Ohio	1
AF-62	Hq. AFCRL, OAR (CRZWD, Irving I. Gringorton) L.G. Hanscom Field Bedford, Massachusetts	1
G-66	Scientific and Technical Information Facility ATTN: NASA Representative (S-AK-DL) P.O. Box 5700 Bethesda, Maryland	1
G-67	Office of Scientific Intelligence Central Intelligence Agency 2430 E Street, N.W. Washington 25, D.C.	1
AR-7	Commanding Officer U.S. Army Research and Development Laboratory Fort Monmouth, New Jersey	1
AR-13	Technical Documents Center Evans Signal Labs. Belmar, New Jersey	1
AR-15	Army Research Office Environmental Research Division 3045 Columbia Pike Arlington 4, Virginia	1
AR-16	Office of the Chief of Research and Dev. Department of the Army The Pentagon Washington 25, D.C.	1

Code	Organization	No. of Copies
F-7	Technical Information Office European Office, Aerospace Research Shell Building, 47 Cantersteen Brussels, Belgium (U)	1
F-50	Defense Research Member Canadian Joint Staff 2450 Massachusetts Ave., N.W. Washington 8, D.C. (U)	2
G-5	Librarian Boulder Laboratories National Bureau of Standards Boulder, Colorado (U)	1
G-21	ASTIA (TIPAA) Arlington Hall Station Arlington 12, Virginia	20
G-34	Documents Expediting Project (Unit X) Library of Congress Washington 25, D.C. (U)	1
G-40	Library National Bureau of Standards Washington 25, D.C. (U)	1
G-41	National Research Council 2101 Constitution Avenue Washington 25, D.C. (U)	1
G-47	Office of Secretary of (DDR and E, Tech. Library) Washington 25, D.C. (U)	1
G-49	Superintendent of Documents Government Printing Office Washington 25, D.C. (U)	1
G-51	Science Advisor Department of State Washington 25, D.C. (U)	1

Code	Organization	No. of Copies
G-52	Director of Meteorological Research U.S. Weather Bureau Washington 25, D.C.	1
G-53	Library U.S. Weather Bureau Washington 25, D.C.	1
I-7	Director, USAF Project RAND The Rand Corporation 1700 Main Street Santa Monica, California Thru A.F. Liaison Office	1
I-8	Dr. William W. Kellogg Rand Corporation 1700 Main Street Santa Monica, California (U)	1
I-40	Institute of Aerospace Sciences, Inc. 2 East 64th Street New York 21, New York (U)	1
I-46	Mr. Malcolm Rigby American Meteorological Society P.O. Box 1736 Washington 13, D.C. (U)	1
N-6	Technical Reports Librarian U.S. Naval Postgraduate School Monterey, California (U)	1
N-16	OAR (Geophysics Code N-416) Office of Naval Research Washington 25, D.C.	1
N-19	Director U.S. Naval Research Laboratory Code 2027 Washington 25, D.C.	1

Code	Organization	No. of Copies
U-1	Library Geophysical Institute University of Alaska P. O. Box 938 College, Alaska (U)	1
U-10	Professor Clarence Palmer Institute of Geophysics University of California Los Angeles 24, California (U)	1
U-13	Dr. Joseph Kaplan Department of Physics University of California Los Angeles, California (U)	1
U-21	Dr. A. M. Peterson Stanford University Stanford, California (U)	1
U-40	Dr. David Fultz Department of Meteorology University of Chicago Chicago, Illinois (U)	1
U-56	Prof. Fred L. Whipple Harvard College Observatory 60 Garden Street Cambridge 38, Massachusetts (U)	1

Remaining copies to:
Hq. AFCRL, OAR (CRFE, Dr. Norman Rosenberg)
L. G. Hanscom Field
Bedford, Massachusetts

General Electric Research Laboratory,
Schenectady, N.Y. PERFORMANCE
CHARACTERISTICS AND EMISSION
COOLING MEASUREMENTS TAKEN ON
A Cs VAPOR THERMIONIC CONVERTER
WITH A THORIUM-TUNGSTEN EMITTER
by J. M. Houston, May 1963 36p. incl.
illus. (Proj. 8659; Task 865902)
(AFCRL-63-450) Scientific Report
[Contract AF-19(604)-8424]
                    Unclassified report

Measurements made on a Cs-vapor
thermionic converter having a 13.3 cm^2
Th-W emitter indicate that in the retarding

(over)

range of the converter the emission cooling
is just what simple theory would predict.
However, for collector-to-emitter voltages
more positive than approximately -1.3 volts,
the emission cooling fell far below that pre-
dicted by simple electron emission from the
emitter, indicating that large amounts of
power (as much as 20 watts/cm^2 at positive
collector voltages) was flowing from the
plasma back to the emitter. This anomaly
in the emission cooling is interpreted in
terms of resonance radiation, excited atoms,
and ions returning to the emitter. These
originate in a region of high electron tem-
perature adjacent to the emitter.